Optical Signal Phase Retrieval with Low Complexity DC-Value Method

Romil K. Patel, *Student member, IEEE*, Isiaka A. Alimi, *Member, IEEE*, Nelson J. Muga, *Member, OSA*, Armando N. Pinto, *Senior Member, IEEE, Member, OSA*

***Abstract*—We propose a novel method to reconstruct the optical signal phase information using direct detection. The method is suitable for minimum phase signals and it enables low complexity, low latency, and low tone power operation. Moreover, the proposed method offers low optical complexity solution for the short-reach links compared with the concurrent phase retrieval techniques. We apply the method to M-ary signals with the transmitted power of as low as 3 dBm, and we are able to reach 70 km for 100 Gb/s quadrature phase shift keying (QPSK) system without optical amplification. Our method is based on the single sideband (SSB) and DC-Value property of the minimum phase signal. The SSB and DC-Value properties are iteratively imposed on the amplitude signal in the frequency domain to recover the full complex field from a directly detected optical signal. The normalized mean square error (NMSE) value between the available amplitude information and reconstructed minimum phase signal amplitude decreases after each iteration, providing global minimum convergence. A constant scaling factor is exploited to improve the convergence speed. The scaling factor provides 6 dB, 4.5 dB, and 2.5 dB error vector magnitude (EVM) gains with 4, 5, and 8 iterations, respectively.**

***Index Terms*—Minimum phase signal, direct detection (DD), iterative reconstruction, carrier to signal power ratio (CSPR).**

I. Introduction

MINIMUM phase signals enable optical field amplitude and phase information retrieval using direct detection [1], [2]. However, minimum phase retrieval based on non-iterative methods tends to require high sampling rates and high tone powers, which consequently leads to the need for high speed digital signal processing (DSP) [3] and induces nonlinear distortions [4], respectively. On the other hand, iterative methods tend to present high latency [5]. To address the aforementioned limitations, a novel low complexity, low latency, and low tone power iterative method is proposed.

Double sideband optical direct detection schemes offer a low cost and simple solution to extract information from an optical signal [6]. However, they impose an irreversible loss of phase information [7]. Single sideband (SSB) methods have been explored to obtain amplitude and phase information using direct detection [8]. However, they tend to suffer a strong penalty due to signal to signal beat interference (SSBI) [8]. The adverse effects of SSBI can be alleviated either by enlarging the band-gap between the carrier and information signal or by increasing the carrier to signal power ratio (CSPR), at the expense of the spectral efficiency [9] or nonlinear signal degradation [10], respectively. Alternative methods to mitigate the effects of SSBI includes the utilization of multi-core fibers and balanced detection [11], [12]. More recently, a minimum phase signal based Kramers-Kronig receiver has been proposed which significantly reduces the impact of SSBI [5], [13]. The minimum phase condition of the signal implies that log-magnitude and phase are related by the Hilbert transform, and this requirement can be fullfilled by adding a constant DC value in the SSB complex signal [14]. However, the nonlinear operations (logarithmic and exponential) in the Kramers-Kronig algorithm demand the DSP to be operated much faster than Nyquist sampling rate to accommodate spectral broadening [4]. To reduce the sampling rate, some approximations have been proposed [15]. Nevertheless, the proposed approximations tend to require higher tone powers which result in an increase of the nonlinear distortions [16]. An upsampling free iterative method based on Hilbert relationship is proposed in [5]. However, this method includes filtering and a nonlinear operation inside the iterative process [5], [17]. In the context of image processing, a phase-retrieval iterative method based on alternate projections on the space-domain and Fourier-domain is proposed in [18]. In [19], the space-domain magnitude initial information is replaced by a non-negativity constraint such that the recovering algorithm relies only on the Fourier magnitude information. Other alternatives to the non-negativity constraint, like steepest-descent, conjugate-gradient, basic input-output, output-output and hybrid input-output algorithms, have also been presented [20]. These methods tend to suffer from slow and local minimum convergence problems [20]. In [21], a Fourier-domain iterative method, which avoids the local minimum problem is proposed, where causality and initial-value condition are imposed in the time-domain.

Starting from the SSB and DC value properties of the minimum phase signal, we develop a novel iterative method to reconstruct the phase of the optical field in direct detection optical communication systems. The proposed method imposes the minimum phase signal property in the frequency domain, which allows the removal of the nonlinear operations in the iterative process, thus reducing significantly the complexity and nonlinear distortions. A constant scaling factor used in

This work was supported in part by Fundação para a Ciência e a Tecnologia (FCT) through national funds, by the European Regional Development Fund (FEDER), through the Competitiveness and Internationalization Operational Programme (COMPETE 2020) of the Portugal 2020 framework, under the projects DSPMetroNet (POCI-01-0145-FEDER-029405) and UID/EEA/50008/2019 (action COHERENTINUOUS).

Romil K. Patel and Armando N. Pinto are with the Department of Electronics, Telecommunications and Informatics, University of Aveiro, and the Instituto de Telecomunicações, Aveiro, Portugal (e-mail: romilkumar@ua.pt; anp@ua.pt).

Isiaka A. Alimi and Nelson J. Muga are with the Instituto de Telecomunicações, Aveiro, Portugal (e-mail: iaalimi@av.it.pt; muga@av.it.pt).

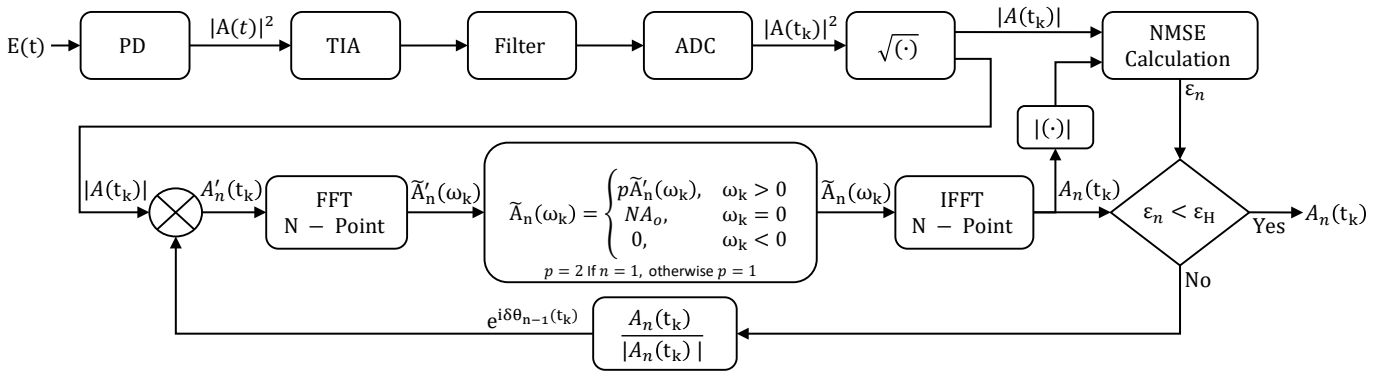

Fig. 1: The schematic of the DC-Value iterative method to reconstruct the full electric field of a minimum phase signal from its intensity information. A constant scaling factor p helps to speed up the convergence process. The process iterates continuously until the NMSE between $|A(t_k)|$ and $|A_n(t_k)|$ becomes less than threshold error ε_H.

the first iteration provides 6 dB, 4.5 dB, and 2.5 dB error vector magnitude (EVM) gains for iteration number 4, 5, and 8, respectively.

Besides the introduction, this paper comprises four sections. In Section II, we describe the proposed DC-Value iterative method. In Sections III and IV, we assess the performance of the proposed method in a scenario without and with noise, respectively. In the last section, we present the major concluding remarks.

II. DC-Value Iterative Method

Figure 1 shows the diagram of the proposed iterative reconstruction method. The complex envelope of the incoming SSB optical signal is $A(t) = A_o + A_s(t)$, where A_o is the complex amplitude of the optical carrier which ensures the DC-Value property, and $A_s(t)$ is the complex SSB signal. When the field is detected using a single photodetector, the generated photocurrent can be expressed as [16],

$$I(t) \propto \left(\underbrace{|A_o|^2}_{\text{DC}} + \underbrace{2\text{Re}\{A_o A_s(t)\}}_{\text{carrier-signal}} + \underbrace{|A_s(t)|^2}_{\text{signal-signal}} \right) \tag{1}$$

where, $\text{Re}\{\cdot\}$ represents the real part of $\{\cdot\}$, the first term, $|A_o|^2$, is the DC component, the second term, $2\text{Re}\{A_o A_s(t)\}$, is the carrier-signal beating, and the last term, $|A_s(t)|^2$, is the signal-signal beating. The photocurrent is then amplified using a transimpedance amplifier (TIA) and filtered by a low pass filter. For simplicity, we consider the photodetector responsivity R and the TIA gain G such that $RG = 1$. Without loss of generality, we assume that A_o is real, i.e. the A_o phase is zero, and the phase of $A_s(t)$ is measured in relation to the phase of A_o. Note that both signals A_o and $A_s(t)$ are supposed to be generated in the transmitter from the same laser and within the laser coherence time. The power of the carrier A_o in relation to the power of the signal defines the carrier to signal power ratio (CSPR). The CSPR is defined as,

$$\text{CSPR} = \frac{|\text{A}_\text{o}|^2}{\langle |\text{A}_\text{s}(\text{t})|^2 \rangle} \tag{3}$$

The current signal is then digitized using an analog to digital converter (ADC) at the frequency that is not less than the Nyquist limit, i.e. 2B, where B is is the photocurrent bandwidth. Afterwards, the square-root operation is carried out to obtain the amplitude $|A(t_k)|$ of the optical field. Taylor series expansion of the nonlinear square root operation can be written as (2), showing the presence of the $\text{Re}\{A(t_k)\}$ term and higher order terms. As evident from (2), the impact of higher order terms can be made less severe by increasing the tone power. After the square root operation, see Fig. 1, the amplitude information signal $|A(t_k)|$ is multiplied by a phase correction factor $e^{i\delta\theta_{n-1}(t_k)}$ which outputs the complex signal $A'_n(t_k)$, where n represents the iteration number. In the first iteration (for $n = 1$), the phase correction factor is assumed to be zero, i.e. $\delta\theta_0(t_k) = 0$. Next, the SSB and DC value properties (see Appendix A and B) of the minimum phase signal are imposed on the Fourier transformed signal $\tilde{A'}_n(\omega_k)$ to attain $\tilde{A}_n(\omega_k)$ as,

$$\tilde{A}_n(\omega_k) = \begin{cases} p\tilde{A'}_n(\omega_k), & \text{for } \omega_k > 0 \\ NA_o, & \text{for } \omega_k = 0 \\ 0, & \text{for } \omega_k < 0 \end{cases} \tag{4}$$

where, N represents the length of the FFT, n represents the iteration number, and p denotes the scaling factor given by,

$$p = \begin{cases} 2, & \text{for } n = 1 \\ 1, & \text{for } n > 1 \end{cases} \tag{5}$$

$$\begin{aligned} |A(t)| &= \sqrt{A_o^2 + 2A_o\text{Re}\{A_s(t)\} + |A_s(t)|^2} \\ &= \text{Re}\{A_s(t)\} + A_o\left[1 + \frac{1}{2}\frac{|A_s(t)|^2}{A_o^2} - \frac{1}{8}\left(\frac{2A_o\text{Re}\{A_s(t)\} + |A_s(t)|^2}{A_o^2}\right)^2 + \frac{1}{16}\left(\frac{2A_o\text{Re}\{A_s(t)\} + |A_s(t)|^2}{A_o^2}\right)^3 - \ldots\right] \end{aligned} \tag{2}$$

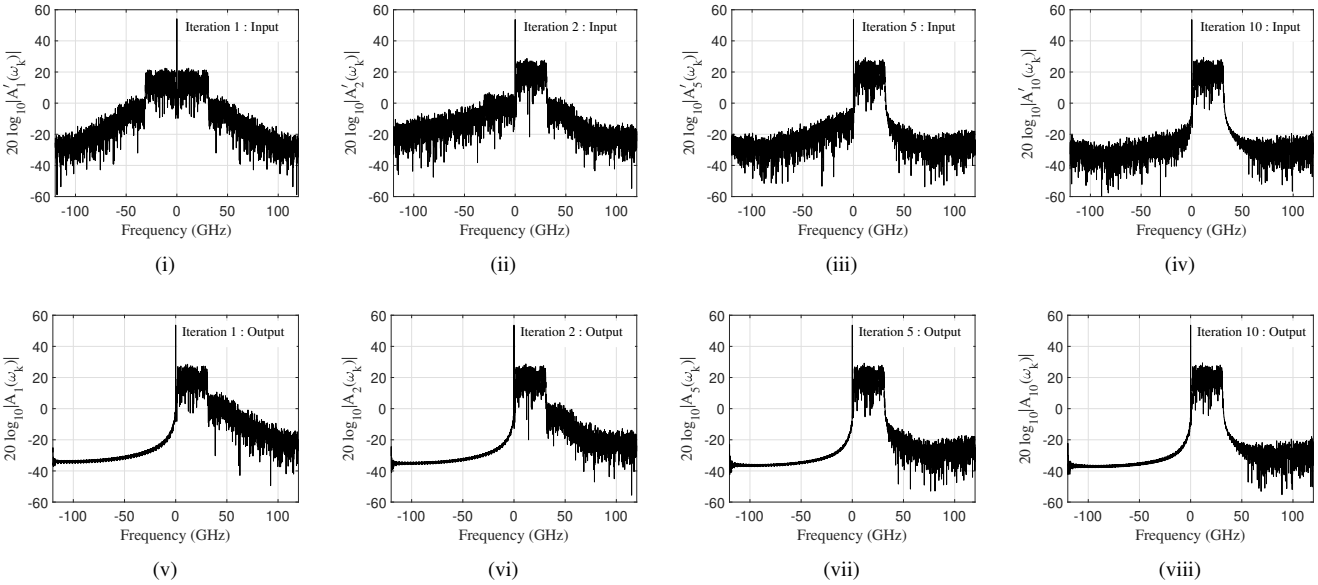

Fig. 2: Magnitude spectrum of the input signal to the proposed method and output minimum phase signal after execution of iteration 1, 2, 5 and 10 with the CSPR of 6 dB. Graphs I, II, III and IV (top-panel) show the spectrum of the input signal $A'_n(t_k)$, and graphs V, VI, VII, and VIII (bottom-panel) show the spectrum of the recovered minimum phase signal $A_n(t_k)$ at the end of iteration number 1, 2, 5, and 10, respectively.

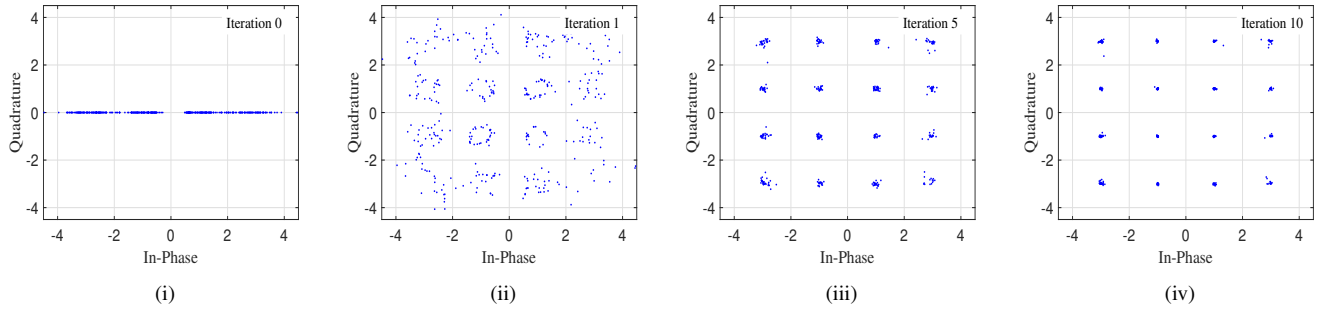

Fig. 3: Recovered IQ constellations of the 30 Gbaud 16QAM signal by the proposed method after the execution of iteration numbers 0, 1, 5 and 10 with the CSPR of 6 dB. After 10 iterations the recovered constellation is very close to the ideal constellation.

The input signal, $A'_n(t_k)$, for the first iteration consists of a real-valued amplitude signal $|A(t_k)|$ (i.e. $\delta\theta_0(t_k) = 0$). The minimum phase condition imposed on the signal forces the negative frequency components to zero and it generates complex-valued signal $A_1(t_k)$ in the time domain (starts acquiring the phase information). As a consequence of forcing negative frequency components to zero, the signal $A_1(t_k)$ will have its real and imaginary parts amplitude scaled by a factor 0.5. Therefore, we set a scaling factor $p = 2$ to adjust the amplitude of the information signal in the first iteration. As shown in the next section, the scaling factor p used in the reconstruction process greatly speed up the convergence process (see Fig. 5). After imposing minimum phase condition, the inverse Fourier transform of the $\tilde{A}_n(\omega_k)$ is computed to obtain $A_n(t_k)$. The normalized mean squared error (NMSE) ε_n between $|A(t_k)|$ and $|A_n(t_k)|$ can be calculated as,

$$\varepsilon_n = \frac{1}{N}\sum_{k=1}^{N} \frac{\Big(|A(t_k)| - |A_n(t_k)|\Big)^2}{\Big(\frac{1}{N}\sum\limits_{k=1}^{N}|A(t_k)|\ \frac{1}{N}\sum\limits_{k=1}^{N}|A_n(t_k)|\Big)} \qquad (6)$$

If the value of the error ε_n is higher than the threshold error ε_H then the updated phase correction vector corresponding to $A_n(t_k)$ can be calculated as $e^{i\delta\theta_n(t_k)} = \frac{A_n(t_k)}{|A_n(t_k)|}$. This phase estimate $e^{i\delta\theta_n(t_k)}$ can be supplied as an updated phase information for the subsequent iteration as shown in Fig.1. This process would repeat continuously until the NMSE ε_n reaches below the threshold ε_H. The NMSE ε_n between the known magnitude $|A(t_k)|$ and the estimated magnitude $|A_n(t_k)|$ is monotonically decreasing after each iteration and has lower bound to zero, therefore, the reconstruction process converges to a limit point.

The convergence process of the proposed DC-Value iterative method is shown in Fig. 2, where the spectrum of the input $A'_n(t_k)$ and the recovered minimum phase signal $A_n(t_k)$ are displayed at the end of iteration number 1, 2, 5, and 10. For the assessment of the convergence process, minimum phase signal $A(t)$ corresponding to 30 Gbaud 16QAM with 6 dB CSPR value is employed in the reconstruction process. For the first iteration, the input signal is $|A(t_k)|\ e^{i\delta\theta_0(t_k)} = |A(t_k)|$ (see Fig. 2(i)) since $e^{i\delta\theta_0(t_k)}$ is an unitary vector, and the corresponding output $A_1(t_k)$, is the first estimation of the

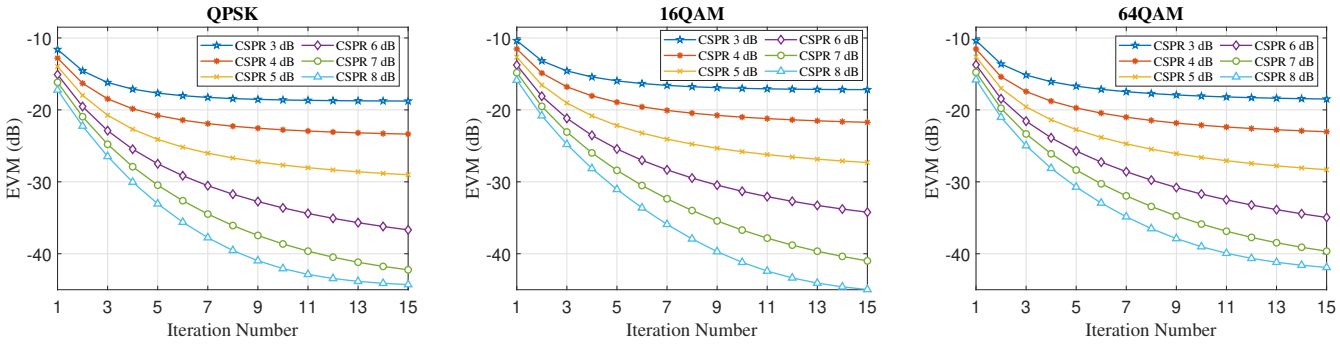

Fig. 4: Error vector magnitude (EVM) versus iteration number of the recovered signal considering different CSPR values, for (i) QPSK, (ii) 16QAM, and (iii) 64QAM signals. Each curve was obtained by varying the DC value to obtain desired CSPR values as shown in the legends.

minimum phase signal as shown in Fig. 2(v). Similarly, input and output corresponding to the second iteration can be given as $|A(t)|\ e^{i\delta\theta_1(t_k)}$ (where $e^{i\delta\theta_1(t_k)} = A_1(t_k)/|A_1(t_k)|$) and $A_2(t_k)$ as shown in Fig. 2(ii) and Fig. 2(vi), respectively. Likewise, the input and output signals at the end of iteration 5 and 10 are shown in Fig. 2(iii) and Fig. 2(vii), and Fig. 2(iv) and Fig. 2(viii), respectively. The accuracy of the signal reconstruction process increases with the number of iterations and high CSPR value.

At the end, the recovered minimum phase signal $A(t_k)$ is passed through the DC remover and then downconverted to recover the 16QAM signal. Figure 3 shows the constellation of the recovered 16QAM signal for the iteration number 0, 1, 5, and 10. For the iteration 1, the input does not contain any phase information i.e. $\delta\theta_0(t_k) = 0$, as shown in Fig. 3(i), and at the end of iteration 1, it starts recovering the phase information as shown in Fig. 3(ii). As it is evident that error in the recovered signal is reduced in the subsequent iterations as shown in Fig. 3(iii) and 3(iv), which display the recovered signal constellation after iteration 5 and 10, respectively. It requires approximately 10 number of iterations to achieve close proximity to the ideal constellation with 6 dB CSPR.

III. Performance Assessment Without Noise

In the following, we assess the performance of the proposed method without noise for different CSPR values and number of iterations for the M-ary modulation formats. For the performance assessment of the method, single-channel 100 Gb/s QPSK, 16QAM, and 64QAM signals with 20% overhead (120 Gb/s) are employed, respectively. At the transmitter side, the complex signals are generated using a raised cosine pulse shaping filter with 0.05 roll-off factor. The complex signal is then multiplied by $e^{i2\pi f t_k}$, i.e. it is upconverted, to generate SSB signal $A_s(t_k)$, where $f \geq B/2$ and B is the bandwidth of the signal. Next, DC value is added to the SSB signal ensuring that real part of the SSB signal becomes non-negative, which generates minimum phase signal $A(t_k)$ in digital domain. The desired CSPR value can be adjusted either by varying DC value or signal power. At the receiver side, the signal is detected using direct detection technique and then processed to recover the full electric field of the minimum phase signal $A(t_k)$ as discussed in section II. The recovered minimum phase signal $A(t_k)$ is passed through DC remover and then downconverted by $e^{-i2\pi f t_k}$ to recover the information signal. The EVM metric is employed to provide a quantitative measure of the recovered signal by the proposed method. The EVM can be estimated as,

$$\text{EVM}_{RMS} = \sqrt{\frac{\sum_{k=1}^{N}((I_k - \tilde{I}_k)^2 + (Q_k - \tilde{Q}_k)^2)}{\sum_{k=1}^{N}(I_k^2 + Q_k^2)}} \tag{7}$$

where, I_k and Q_k represent the in-phase and quadrature samples of the k^{th} transmitted symbol, respectively, and $\tilde{I}_k$ and $\tilde{Q}_k$ represent the in-phase and quadrature samples of the k^{th} recovered symbol, respectively, and N represents the length of the sequence. For the performance assessment, CSPR values of 3 dB, 4 dB, 5 dB, 6 dB, 7 dB, and 8 dB are employed and the reconstruction process is iterated for 15 iterations to recover the minimum phase signal. The EVM of the recovered QPSK, 16QAM and 64QAM signals after execution of each iteration for different CSPR values are displayed in Fig. 4(i), Fig. 4(ii), and Fig. 4(iii), respectively. It is shown that the EVM value improves after execution of each

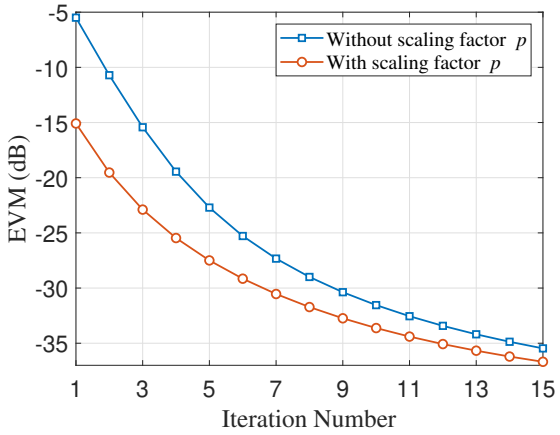

Fig. 5: Comparison of EVM without and with scaling factor p for the QPSK signal.

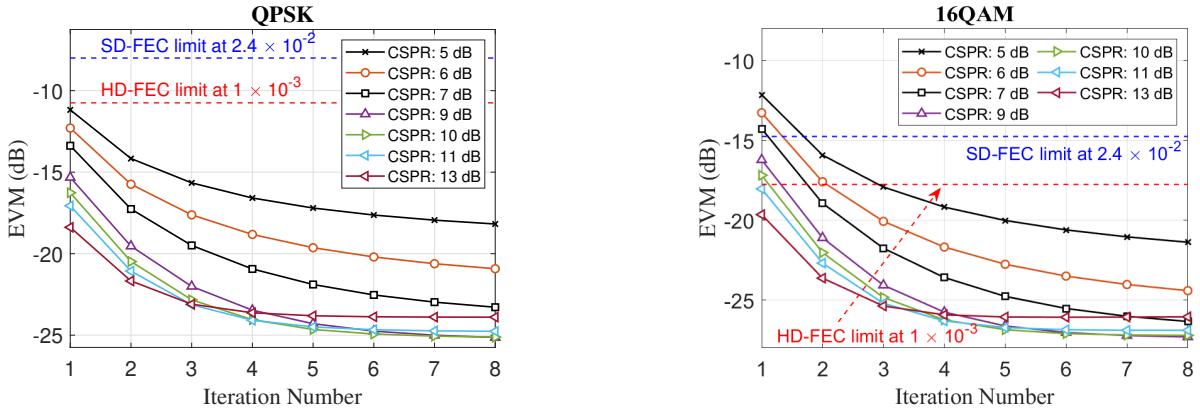

Fig. 6: EVM of the recovered signal using the DC-Value iterative method after 20 km of SSMF with 3 dBm transmitted power. Blue and red dashed lines show the corresponding SD-FEC and HD-FEC limits, respectively.

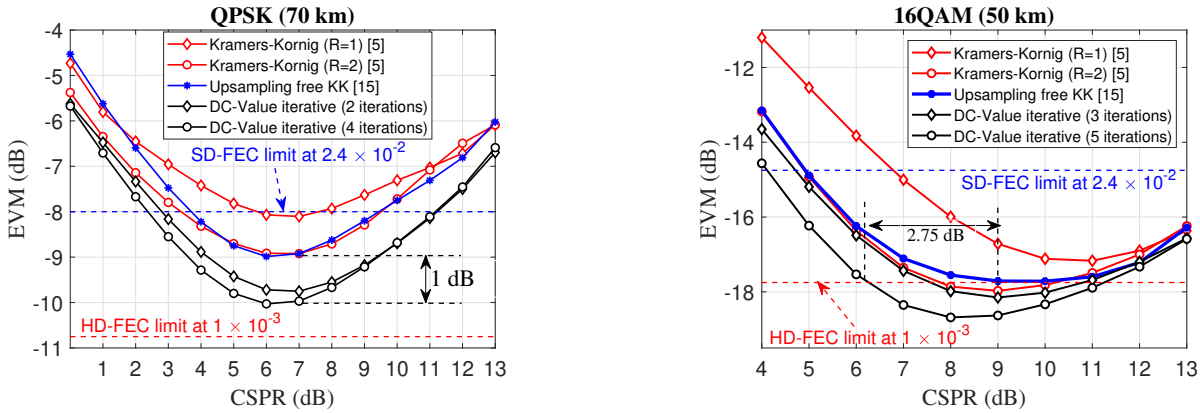

Fig. 7: EVM of the recovered signal for the (i) QPSK (70 km), and (ii) 16QAM (50 km) signals with 3 dBm transmitted power. R denotes the upsampling factor used in the Kramers-Kronig method. Blue and red dashed lines show the corresponding SD-FEC and HD-FEC limits, respectively.

iteration, providing global minimum convergence. Without noise, the reconstruction process improves with the increase of the CSPR and the number of iterations. In the following, we discuss the impact of the inclusion of the scaling factor. Figure 5 shows the EVM values of the recovered signal by the proposed method with and without scaling factor p. The figure shows that implementation of the scaling factor provides approximately 6 dB, 4.5 dB, and 2.5 dB EVM gains for iteration number 4, 5, and 8, respectively. This shows that there is a considerable increase in the EVM gain with low number of iterations with the implementation of the scaling factor. Alternatively, the employed scaling factor helps in enhancing the system convergence by reducing the required numbers of iterations n by 2. That is, instead of n iterations we need $n-2$ iterations. For simplicity and clarity, we present the results that are based on the QPSK implementation. However, it should be noted that the offered advantages of the scaling factor are also applicable to other modulation formats (i.e. 16QAM and 64QAM). It should also be noted that the scaling factor p is only different from 1 in the first iteration, therefore the condition for global minimum convergences is always satisfied, see Appendix B.

IV. Performance Assessment in Presence of Noise

This section shows the simulation analysis of the proposed method in the presence of noise using an in-house C++/MATLAB simulator, named NetXpto-LinkPlanner, developed by the researchers and Ph.D. students of the Instituto de Telecomunicações over the years. At the transmitter, the signal is modulated using a Mach-Zehnder IQ modulator operating in its linear regime. For optical signal transmission, we chose a standard single-mode fiber (SSMF) with an attenuation of 0.2 dB/km, chromatic dispersion of 17 ps/nm/km, and nonlinear coefficient $\gamma = 0.0014$ W^{-1}m^{-1}. Inside the fiber, the waveform evolution is calculated by using the split-step Fourier method with a step-size of 1 km, taking into consideration that we are operating in a quasi-linear regime. Also, we limit the launch power to 3 dBm for a quasi-linear operation regime. As we have considered short-reach links, the polarization-mode-dispersion (PMD) effects are negligible [22]. Since no optical pre-amplifier is used prior to photodetection, the incident optical power on the photodetector is low and the shot noise contribution is negligible, thus making the system performance essentially limited by the thermal noise. For the analysis, we have considered the input-referred noise

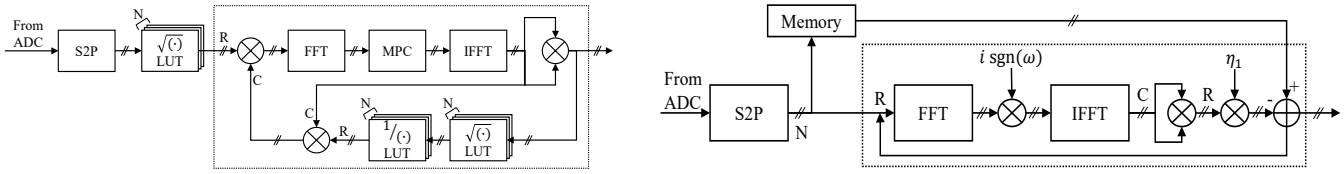

Fig. 8: Hardware implementation scheme of (i) DC-Value iterative method, (ii) iterative linear filter. S2P: Serial-to-parallel, MPC: Minimum phase condition, SF: Sideband filter R: Real signal, C: Complex signal, N: Number of points (Parallelization), dotted boxes show the iterations.

TABLE I: COMPUTATIONAL COMPLEXITY COMPARISON

	Kramers-Kronig [5]	**Iterative linear filter [13]**	**Proposed DC-Value iterative**
Number of multiplier	$(3\mathrm{N_s}+\mathrm{N_h}/2+2)\mathrm{RN}$	$(4\mathrm{Nlog_2N}+3\mathrm{N})\mathrm{k}$	$(4\mathrm{Nlog_2N}+6\mathrm{N})\mathrm{k}$
Number of adder	$(3\mathrm{N_s}+\mathrm{N_h}/2)\mathrm{RN}$	$(4\mathrm{Nlog_2N}+\mathrm{N})\mathrm{k}+\mathrm{N}$	$(4\mathrm{Nlog_2N}+\mathrm{N})\mathrm{k}$
Memory	$16\mathrm{RN}^{\dagger}$	$8\mathrm{N}^{\bullet}$	$12\mathrm{N}^{\dagger}$

*k: Number of iterations; *R: Upsampling factor; †: kbits; $^{\bullet}$: bits

current spectral density of 30 $\mathrm{pA}/\sqrt{\mathrm{Hz}}$ [22] and an ADC with 8-bit vertical resolution. Notice that, the ADC noise is also negligible considering the thermal noise in the receiver.

Figure 6 shows the EVM of the recovered QPSK and 16QAM signals after 20 km of SSMF for different CSPR values. It shows that SSBI becomes more severe and degrade the quality of recovered signal at low CSPR ratios. Contrarily, very high CSPR would deteriorate the SNR (sensitivity penalty) at the receiver end, which limits the system performance. Figure 6 shows that irrespective of the modulation formats, EVM is decreasing after each iteration.

The iterative technique based on the linear filtering discussed in [13] works by calculating SSBI terms and subtracting them from the detected signal. However, due to the inaccuracy of the SSBI approximation caused by the introduction of additional distortion by the linear filters, this technique has the drawback of limited effectiveness. It is shown that Kramers-Kronig provides better SSBI compensation effectiveness over iterative linear filtering methods [13]. Therefore, we present a comparative analysis of the proposed DC-Value iterative with the Kramers-Kronig [5] and the upsampling free Kramers-Kronig [15] methods. Figure 7 shows the EVM of the recovered signal by the Kramers-Kronig, the upsampling free Kramers-Kronig, and the proposed DC-Value iterative methods for the QPSK and 16QAM signals after 70 km and 50 km SSMF, respectively. We compare the results of the Kramers-kronig ($R=1$ and $R=2$) [5] , upsampling free Kramers-Kronig [15], and proposed DC-value iterative method. Figure 7(i) shows that $\sim$1 dB EVM gain is achieved over Kramers-kronig ($R=2$) and upsampling free Kramers-Kronig ($R=1$) after the 4 iterations. Similarly, in 16QAM (see Fig. 7(ii)), the DC-value iterative method requires $\sim$2.75 dB less CSPR to surpasses the accuracy of the Kramers-Kronig ($R=2$) and upsampling free Kramers-Kronig with 3 iterations.

A. Computational Complexity Analysis

In this subsection, we analyze the computational complexity of the proposed method and present a comprehensive comparison with the Kramers-Kronig [5] and the iterative linear filter [13] methods. Considering a DSP chip low clock frequency, f_{clock}, parallelization is employed to realize a high sampling frequency, f_s. The degree of parallelization is determined by the $N=\lceil f_s/f_{clock}\rceil$, where $\lceil\cdot\rceil$ is the ceiling operator. Considering the ADC with an 8-bit resolution, it requires 4 kbits memory to fill each lookup table (LUT) with 2-byte floating-point number ($2^8\times 2^4$). For an efficient FFT implementation, we set the degree of parallelization to $N=2^m$, where $m>1$. The Kramers-Kronig requires digital signal upsampling and downsampling, which can be realized by an N_s tap FIR filter. The Hilbert transformation in the Kramers-Kronig method can be implemented using an FIR filter having N_h taps. This Hilbert filter requires $N_h/2$ real-valued adders and $N_h/2$ real-valued multipliers [4].

Figure 8(i) shows the schematic of the hardware implementation for the proposed iterative method. First, a serial to parallel (S2P) process is carried out to realize the parallelization, followed by a square-root operation. Next, the magnitude is multiplied with the complex phase correction factor which requires $2N$ real multiplications. Following that, FFT is calculated requiring $\frac{N}{2}\mathrm{log_2N}$ complex multiplications (i.e. 4 real multiplications and 2 real additions) and $N\mathrm{log_2N}$ complex additions (i.e. 2 real additions). For the minimum phase condition, the scaling factor implementation can be implemented by 1-bit shift operation. Afterwards, IFFT requires the same complexity as FFT. Next, the phase correction factor is calculated by taking $|(\cdot)|^2$ (i.e. $2N$ real multiplications and N addition), followed by a square-root, an inverse and a multiplication (i.e $2N$ real multiplication) operation. Similarly, we estimate the complexity for the iterative linear filter method shown in Fig. 8(ii). In iterative linear filter method, the sideband filter includes a multiplication by 2 operation which can be implemented by 1-bit shift operation. The estimated

computational complexity comparison of three methods (the Kramers-Kronig [5], the iterative linear filter [13], and the DC-Value iterative proposed here) is presented in Table I.

The required computational complexity increases linearly with the sampling frequency f_s since higher degree of parallelization N is required to to realize high f_s when f_{clock} is fixed. Considering both N_h and N_s with 128 taps, $N = 256$, $R = 2$, $k = 5$, and $f_{clock} = 200$ MHz, Kramers-Kronig method requires $\sim 10^5$ real-valued adders and multipliers, where this number would be reduced to $\sim 4.5 \times 10^4$ for both iterative linear filter method and proposed iterative method, respectively. Despite the FFT/IFFT pairs are involved, the proposed method exhibits low latency since it requires less number of multipliers and adders operation to be performed compared to Kramers-Kronig algorithm. Also, the proposed DC-Value iterative method enables higher accurate reconstruction with low CSPR requirement (no extra receiver sensitivity penalty unlike [4]) without the need for digital upsampling.

V. Conclusion

Using the SSB and DC-Value properties of the minimum phase signal, we have proposed an iterative method which reconstructs the full electric field minimum phase signal from its amplitude information in direct detection optical systems. The proposed reconstruction technique does not contain nonlinear operations. This ensures upsampling free reconstruction process at low tone power (low CSPR) operation. Moreover, we have shown that a constant scaling factor p used in the iterative process speeds up the convergence process. Also, we have performed a simulation analysis of a 100 Gb/s (120 Gb/s system with 20% overhead). Results show that the proposed technique provides $\sim$1 dB EVM gain when compared with the Kramers-kronig method for a QPSK signal after 70 km of SSMF transmission. Besides, regarding the 16QAM signal, the proposed technique requires $\sim$2.75 dB lesser tone power to surpass the accuracy of the other two methods, with as low as 3 iterations. The presented results show that the proposed technique presents salient features that can facilitate effective field reconstruction, making it a promising technique in the direct detection based optical communication systems.

Appendix A
Minimum Phase Signal

The signal, whose logarithm is analytic in the upper half of complex z plane with $z = t + i\tau$ can be given as,

$$A(t) = A_o + A_s(t) \tag{8}$$

where $A(t)$ is a minimum phase signal in which $|A_s(t)|$ is the SSB signal and a constant $A_o > |A_s(t)|$. The analytic signal vanish at the extremities of the upper half of the complex z plane which can be viewed from the (8) as,

$$A(z) = A_o\left[1 + \frac{A_s(z)}{A_o}\right] \tag{9}$$

Since $A(z)$ is Fourier transformable,

$$\ln\{\tilde{A}(0)\} = \lim_{z\to\infty} \ln\{A(z)\} = \ln\{A_o\},\ for\ \tau \geq 0. \tag{10}$$

$$\lim_{z\to\infty} \ln\left[\frac{A(z)}{A_o}\right] = 0,\ for\ \tau \geq 0. \tag{11}$$

where $\tilde{A}(\omega)$ is the Fourier transform of $A(z)$. Therefore, the necessary and sufficient condition of minimum phase signal includes (i) the analyticity (i.e. $\tilde{A}(\omega) = 0$) for $\omega < 0$, and (ii) DC-Value property $\tilde{A}(0) = A_o$ in the frequency domain which can be used to develop an iterative algorithm to reconstruct the minimum phase signal from its magnitude information.

Appendix B
NMSE Reduction

Consider an error function, E_n, as the mean squared error between known magnitude, $|A(t_k)|$, and the estimate magnitude, $|A_n(t_k)|$, on each iterations as,

$$E_n = \sum_{k=0}^{N-1} \Big|\ |A(t_k)| - |A_n(t_k)|\ \Big|^2 \tag{12}$$

where N is the number of samples. Following [21], we show that the error function is a monotonically decreasing function. Consider the identity $|e^{[i\delta\theta_n(t_k)]}|^2 = 1$ to express (12) as,

$$E_n = \sum_{k=0}^{N-1} \Big|\ |A(t_k)|e^{(i\delta\theta_n(t_k))} - |A_n(t_k)|e^{(i\delta\theta_n(t_k))}\Big|^2$$

$$E_n = \sum_{k=0}^{N-1} |A'_n(t_k) - \tilde{A}_n(t_k)|^2 \tag{13}$$

From the Parseval's theorem (13) can be given in frequency domain as,

$$E_n = \frac{1}{N}\sum_{k=0}^{N-1} |\tilde{A'}_n(\omega_k) - \tilde{A}_n(\omega_k)|^2 \tag{14}$$

where $\tilde{A'}_n(\omega_k)$ and $\tilde{A}_n(\omega_k)$ are the FFT of $A'_n(t_k)$ and $\tilde{A}_n(t_k)$, respectively. From the minimum phase condition, it follows that, for $\omega_k > 0$,

$$|\tilde{A'}_n(\omega_k) - \tilde{A}_n(\omega_k)|^2 \geq |\tilde{A'}_n(\omega_k) - \tilde{A}_{n+1}(\omega_k)|^2 = 0 \tag{15}$$

and for $\omega_k \leq 0$,

$$|\tilde{A'}_n(\omega_k) - \tilde{A}_n(\omega_k)|^2 = |\tilde{A'}_n(\omega_k) - \tilde{A}_{n+1}(\omega_k)|^2. \tag{16}$$

Summing (15) and (16) over all ω_k, we get,

$$E_n = |\tilde{A'}_n(\omega_k) - \tilde{A}_n(\omega_k)|^2 \geq |\tilde{A'}_n(\omega_k) - \tilde{A}_{n+1}(\omega_k)|^2 \tag{17}$$

Therefore, from Parseval's theorem, and (17),

$$E_n \geq \frac{1}{N}\sum_{k=0}^{N-1} |\tilde{A'}_n(\omega_k) - \tilde{A}_{n+1}(\omega_k)|^2$$

$$E_n \geq \sum_{k=0}^{N-1} \Big|\ |A(t_k)| - |A_{n+1}(t_k)|\ \Big|^2 = E_{n+1} \tag{18}$$

Thus, E_n is a monotonically decreasing function.

REFERENCES

[1] A. Mecozzi, "Retrieving the Full Optical Response from Amplitude Data by Hilbert Transform," *Optics Communications*, vol. 282, no. 20, pp. 4183 – 4187, 2009.

[2] D. Cassioli and A. Mecozzi, "Minimum-phase impulse response channels," *IEEE Transactions on Communications*, vol. 57, no. 12, pp. 3529–3532, December 2009.

[3] X. Chen, C. Antonelli, S. Chandrasekhar, G. Raybon, A. Mecozzi, M. Shtaif, and P. Winzer, "Kramers–kronig receivers for 100-km datacenter interconnects," *Journal of Lightwave Technology*, vol. 36, no. 1, pp. 79–89, Jan 2018.

[4] T. Bo and H. Kim, "Towards Practical Kramers-Kronig Receiver: Resampling, Performance, and Implementation," *Journal of Lightwave Technology*, pp. 1–1, 2018.

[5] A. Mecozzi, C. Antonelli, and M. Shtaif, "Kramers-Kronig Coherent Receiver," *Optica*, vol. 3, no. 11, pp. 1220–1227, Nov 2016.

[6] J. Cartledge and A. Karar, "100 Gb/s Intensity Modulation and Direct Detection," *Journal of Lightwave Technology*, vol. 32, no. 16, pp. 2809–2814, Aug 2014.

[7] E. Ip, A. Lau, D. Barros, and J. Kahn, "Coherent Detection in Optical Fiber Systems," *Opt. Express*, vol. 16, no. 2, pp. 753–791, Jan 2008.

[8] Z. Li, M. Erkılınç, S. Pachnicke, H. Griesser, B. Thomsen, P. Bayvel, and R. Killey, "Direct-Detection 16-QAM Nyquist-Shaped Subcarrier Modulation with SSBI Mitigation," *IEEE International Conference on Communications*, pp. 5204–5209, June 2015.

[9] A. Lowery and J. Armstrong, "Orthogonal-Frequency-Division Multiplexing for Dispersion Compensation of Long-haul Optical Systems," *Opt. Express*, vol. 14, no. 6, pp. 2079–2084, Mar 2006.

[10] S. Randel, D. Pilori, S. Chandrasekhar, G. Raybon, and P. Winzer, "100-Gb/s Discrete-Multitone Transmission Over 80-km SSMF Using Single-Sideband Modulation with Novel Interference-Cancellation Scheme," *2015 European Conference on Optical Communication (ECOC)*, pp. 1–3, Sept 2015.

[11] Y. Wang, Z. Wang, Y. Shen, W. Liu, S. You, X. Li, M. Luo, and Q. Yang, "Beyond 100-Gb/s Single-Sideband Direct Detection Using Multi-core Fiber and SSBI Elimination," in *Opto-Electronics and Communications Conference (OECC) and Photonics Global Conference (PGC)*, July 2017, pp. 1–3.

[12] J. Ma, "Simple Signal-to-Signal Beat Interference Cancellation Receiver Based on Balanced Detection for a Single-Sideband Optical OFDM Signal with a Reduced Guard Band," *Opt. Lett.*, vol. 38, no. 21, pp. 4335–4338, Nov 2013.

[13] Z. Li, M. Erkılınç, K. Shi, E. Sillekens, L. Galdino, B. Thomsen, P. Bayvel, and R. Killey, "SSBI Mitigation and the Kramers–Kronig Scheme in Single-Sideband Direct-Detection Transmission With Receiver-Based Electronic Dispersion Compensation," *Journal of Lightwave Technology*, vol. 35, no. 10, pp. 1887–1893, May 2017.

[14] A. Oppenheim and R. Schafer, *Digital Signal Processing*. Prentice-Hall, 1975.

[15] T. Bo, "Kramers-kronig receiver without digital upsampling," in *2018 Optical Fiber Communications Conference and Exposition (OFC)*, March 2018, pp. 1–3.

[16] T. Bo and H. Kim, "Kramers-Kronig Receiver Operable Without Digital Upsampling," *Opt. Express*, vol. 26, no. 11, pp. 13 810–13 818, May 2018.

[17] N. J. Muga, R. K. Patel, I. A. Alimi, N. A. Silva, and A. N. Pinto, "Self-coherent optical detection for access and metro networks," in *2019 21st International Conference on Transparent Optical Networks (ICTON)*, July 2019, pp. 1–4.

[18] R. W. Gerchberg and W. O. Saxton, "A Practical Algorithm for the Determination of Phase from Image and Diffraction Plane Pictures," *Opt. Lett.*, vol. 35, no. 2, pp. 237–250, Nov 1972.

[19] J. R. Fienup, "Reconstruction of an object from the modulus of its Fourier transform," *Opt. Lett.*, vol. 3, no. 1, pp. 27–29, Jul 1978.

[20] J. Fienup, "Phase Retrieval Algorithms: A Comparison," *Appl. Opt.*, vol. 21, no. 15, pp. 2758–2769, Aug 1982.

[21] T. Quatieri and A. Oppenheim, "Iterative Techniques for Minimum Phase Signal Reconstruction from Phase or Magnitude," *IEEE Transactions on Acoustics, Speech, and Signal Processing*, vol. 29, no. 6, pp. 1187–1193, December 1981.

[22] J. K. Perin, A. Shastri, and J. M. Kahn, "Design of low-power dsp-free coherent receivers for data center links," *Journal of Lightwave Technology*, vol. 35, no. 21, pp. 4650–4662, Nov 2017.